

Fabrication and optical characterization of thin two-dimensional Si₃N₄ waveguides

N. Daldosso^{a,*}, M. Melchiorri^a, F. Riboli^a, F. Sbrana^a, L. Pavesi^a, G. Pucker^b, C. Kompocholis^b, M. Crivellari^b, P. Bellutti^b, A. Lui^b

^aDepartment of Physics, Università di Trento, via Sommarive 14, I-38050 Povo, Trento, Italy

^bIstituto Trentino di Cultura, Centro per la Ricerca Scientifica e Tecnologica, Microsystem Division, via Sommarive 18, I-38050 Povo, Trento, Italy

Available online 18 October 2004

Abstract

In view of the integration within Si-based optical devices, LPCVD (low-pressure chemical vapor deposition) thin-film Si₃N₄ waveguides have been fabricated on a Si substrate within a CMOS fabrication pilot-line. Different structures (channel, rib and strip-loaded) were designed, fabricated and characterized both optically and structurally to optimize waveguide performances. Geometry, sidewall as well as layer roughness of the waveguides have been investigated by scanning electron microscopy and atomic force microscopy. Optical guided modes have been observed and propagation loss measurements at 632.8 and 780 nm have been performed by using the cut-back technique, the insertion loss technique and scattered light collection. The channel waveguides have shown propagation losses of about 0.1–0.2 dB/cm. Differences between geometries and lithographic processes have been discussed. Polarization dependence of propagation losses has been investigated too.

Optical guided modes have also been measured in the near-infrared range (at 1544 nm), where propagation losses are about 4.5–5 dB/cm, quite larger with respect to the visible, because of the poorer confinement factor of the optical modes.

© 2004 Elsevier Ltd. All rights reserved.

Keywords: Complementary metal-oxide-semiconductor (CMOS)-compatible technology; Optical propagation losses; Silicon nitride; Silicon-integrated photonics; Waveguides

1. Introduction

In recent years some concerns related to fundamental materials and processing aspects about the evolution of microelectronics have been raised [1]. For example, as the integration is progressing the length of the interconnects on a single chip is getting longer and more complex. Nowadays chips have total interconnection

length per unit area of the chip of some 5 km/cm² with a chip area of 450 mm². This results in device limitations in terms of speed, packaging and power dissipation [2]. A possible solution could be the use of optical interconnects [3]. Till now, various passive optical components have been developed for WDM-based photonic networks [4]; however, most of these are not compatible with silicon technology. Hybrid technology makes the system fabrication difficult and costly because different materials have to be assembled in a unique device. Silicon microphotonics, which merges photonics and silicon microelectronic components, might reduce

*Corresponding author. Tel.: +39-0461-881541; fax: +39-0461-881696.

E-mail address: daldosso@science.unitn.it (N. Daldosso).

the cost of production and improve the integrability of a device [5,6]. It is predicted that optical interconnects will be used to connect computer boards in few years, while the use of optical interconnects within the chip will possibly be realized in 10–15 years from now [7].

The first component ubiquitous in silicon microphotonics is the optical waveguide, which is used to channel light signal in the system. A natural choice is to look for some of the commonly used dielectrics in microelectronics. Thin waveguides with Si_3N_4 core surrounded by SiO_2 cladding layers represent one of the best solutions to have large refractive index difference ($\Delta n \cong 0.55$), low scattering losses, no absorption losses and compatibility with Si technology. Various low-loss optical waveguides, produced by different techniques, have been reported in the last 30 years [8–15], and some applications in optical devices have been already demonstrated [16–18]. However, it was shown that Si_3N_4 waveguides present remarkable losses due to the vibrational overtones of Si–H and N–H bonds, thus preventing competitive waveguides for the third telecom window [10,14].

In this paper, we report on the systematic fabrication and characterization of low-loss $\text{Si}_3\text{N}_4/\text{SiO}_2$ waveguides produced within a CMOS fabrication pilot-line by low-pressure chemical vapor deposition (LPCVD). The use of LPCVD reduces interface roughness and consequently the related scattering losses. We investigated the optical properties of thin-film Si_3N_4 waveguides deposited on Si substrate as a function of the waveguide geometry and fabrication technology by using visible and infrared light. Three kinds of waveguides were designed, fabricated and characterized: rib, channel and strip-loaded.

2. Experimental

In CMOS fabrication, silicon nitride is either deposited by using LPCVD (at 700–800 °C) or by plasma-enhanced chemical vapor deposition (PECVD, at 200–400 °C). Stoichiometric Si_3N_4 has negligible absorption losses and quite large refractive index (2.01 at 780 nm) and is therefore, nearly an ideal material for the guiding layer. A problem for waveguide fabrication is the high tensile stress of such LPCVD silicon nitride films (1.3 GPa for the Si_3N_4 used in this study), which limits the maximum film thickness to approximately 250 nm—thicker films tend to crack. Propagation losses are essentially related to *scattering losses* and to *leakage losses* towards the Si substrate. Leakage losses towards the Si substrate have been avoided by growing a sufficiently thick layer of SiO_2 (2.0 μm). Since the sidewall roughness and geometry significantly influence the propagation properties, we tested different etching processes for waveguide definition (chemical etching with H_3PO_4 and two different plasma etching processes).

However, the relatively large width (about 10 μm) reduces scattering losses due to irregularity of lateral edges of the mesa structures.

The fabrication process is briefly summarized in the following: a 2.0 μm cladding layer of boron–phosphor–silicate glass was deposited on the Si substrates. The silicon nitride guiding layer of 200 nm was deposited by a LPCVD process and the two-dimensional (2-D) rectangular waveguides were defined by lithography and etching. In this way we obtain rib geometry. Channel waveguides were obtained from rib-waveguides by covering the rib with a 520 nm layer of a medium-temperature LPCVD TEOS SiO_2 (SiO_2 precursor: *tetraethyl orthosilicate*) top cladding. In case of the channel waveguides the rib was defined either with the silicon nitride plasma etcher (i.e. sample G3) or with an oxide plasma etcher (i.e. sample G4). For the strip-loaded waveguides, both chemical (wet) and plasma (dry) etching were used to define the loading 520 nm thick layer of SiO_2 strip over the Si_3N_4 layer. Wet-etching was done with BHF 7:1 (buffered HF); etching process stops exactly at the $\text{SiO}_2/\text{Si}_3\text{N}_4$ interface (i.e. sample G5). Plasma oxide etching was also attempted using a fixed time (i.e. sample G6). The selectivity between $\text{SiO}_2/\text{Si}_3\text{N}_4$ is low. Optical interference and SEM analysis show that besides removing the SiO_2 layer about 30 nm of Si_3N_4 was removed also.

To improve the facets of the waveguides, we defined them by a dry-etching process and then the edges of the Si substrates were removed by anisotropic wet-etching with TMAH (tetramethyl-ammonium-hydroxide). This procedure simplifies the coupling of the light and reduces insertion losses. A scanning electron microscopy (SEM) image of a typical facet obtained with this procedure together with a scheme is given in Fig. 1.

SEM has been employed to check the deposition and etching processes by investigating geometry, sidewall as well as layer roughness of the different waveguides structures.

Atomic force microscopy (AFM) has been used to characterize the morphologic structure of the waveguides. AFM imaging was performed in tapping mode in the air by using a Si non-contact mode cantilever with a resonant frequency of 210 kHz. Prior to use, the piezoelectric scanner was calibrated by using reference standard grating. As an example (sample G1), a 27.6 $\mu\text{m} \times 27.6 \mu\text{m}$, 512 \times 512 pixel, air AFM image of the surface of channel waveguide is shown in Fig. 2. The cross section profile taken along the line indicated on the AFM image allows to appreciate and estimate the lateral dimension and the height of the waveguide. The lateral dimension is about 12.8 μm . The large measured height (about 490 nm) is due to the fact that an over-etching of the SiO_2 bottom cladding occurred because of the non-perfect calibration of the oxide plasma etching. This over-etching was documented also by SEM images.

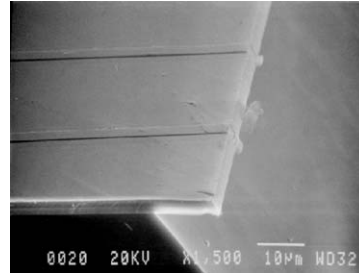
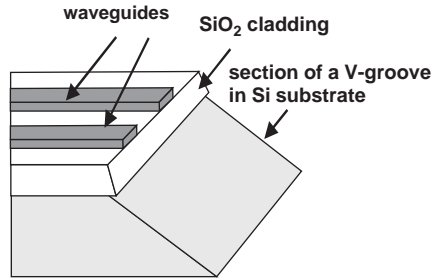


Fig. 1. Scheme and SEM image of the facets of the silicon-nitride waveguides defined by a combination of plasma etching and anisotropic etching with TMAH.

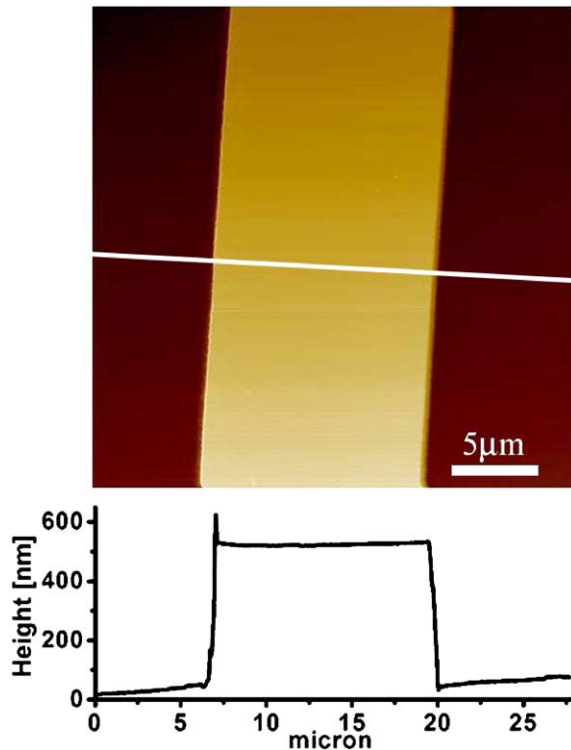


Fig. 2. Room temperature air AFM image of G1 sample. Image size is $27.6\mu\text{m} \times 27.6\mu\text{m}$, 512×512 pixel. Cross section line profile taken along the line indicated on the AFM image.

Propagation loss measurements have been performed by using the cut-back, light scattering (top-view) and insertion losses technique. In the cut-back technique, waveguides have been cleaved at different lengths and the intensity of the transmitted light has been measured. The top-view technique is based on the assumption that the scattered light intensity observed from the top of the waveguide is representative of the attenuation of the optical mode propagating along the waveguide's length. The decrease of the top scattered light can be easily detected by looking at the surface of the waveguide with

a camera. The insertion loss technique is based on the measurement of the power transmitted from the waveguide output facet as a function of the input power. This technique can be useful to estimate the propagation loss through the waveguide, once coupling losses have been estimated and/or calculated. Average of multiple measurements (from 5 to 30) on different waveguides are always reported for each technique.

Waveguides have been measured by coupling-in light from a laser diode (780 nm—10 mW or 1544 nm—5 mW of power) through an objective ($40\times$) or a single-mode tapered fiber and coupling-out the light with microscope objective ($40\times$) matched to a zoom mounted on a high-performance CCD (or InGaAs) camera. Nano-positioning stages are used to efficiently inject the light within the thin waveguide. A prism beam splitter allows dividing the transmitted light in two parts: one is directed to the CCD (or InGaAs) camera, the other is directed to a calibrated Si photodiode (or Ge detector) which yields intensity measurements of the transmitted light. Top-view observation is performed by means of an optical microscope and a CCD (or InGaAs) camera mounted on top of the measuring system.

3. Results and discussion

Fig. 3 shows an example of the transmittance measured by the cut-back technique at 780 nm for the strip-loaded sample G6. Data (reported in natural logarithmic scale) show linear behavior. The linear fit results in a propagation loss coefficient of about 1.5 ± 0.2 dB/cm. It is worth noting that fitting either the averaged values or the maximum values results in the same loss coefficient. Propagation loss coefficients have been obtained also by the top-view technique. Fig. 4 reports the data for the channel waveguide G3 at 780 nm. Scattered intensity is given in natural logarithmic scale. A linear fit of the data yields a propagation loss coefficient of 0.1 ± 0.05 dB/cm. Table 1 presents the propagation loss coefficients of the different samples. Values obtained by the two different techniques are in

good agreement. This is quite important in establishing a good practise. The cut-back technique appears to be more correct, but it is sample and time consuming

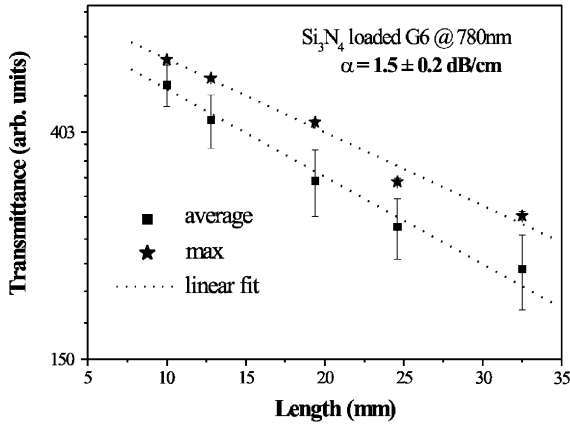


Fig. 3. Transmittance measurements as a function of sample length (cut-back technique) of a strip-loaded waveguide (sample G6) at 780 nm. The propagation loss coefficient is 1.5 ± 0.2 dB/cm.

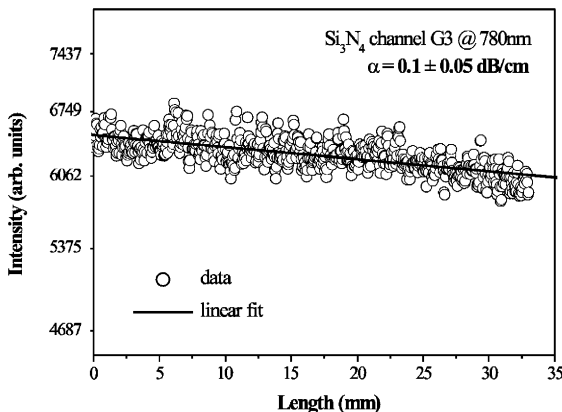


Fig. 4. Scattered light intensity (top-view measurements) along the sample length of a channel waveguide (sample G3) at 780 nm. The propagation loss coefficient is 0.1 ± 0.05 dB/cm.

because of the needs of reproducible coupling conditions, good waveguide facets and long measurement times. The top-view method, once validated against the cut-back method, is very simple and rapid.

From Table 1, significant differences between the various samples can be observed. Channel waveguides show low propagation losses, whereas rib and strip-loaded waveguides present one order of magnitude larger losses at 780 nm. The quite large loss-value of rib waveguides (sample G1) is probably due to the fact that the guiding layer is directly exposed to the air, thus enhancing scattering losses due to roughness and defects on the top surface. Propagation losses of strip-loaded waveguides (G5 and G6) are comparable to the corresponding planar waveguides (about 1.5–2 dB/cm). This is in agreement with the fact that the highest optical modes are not well-confined and extend through the planar core. Channel waveguides (G3 and G4) present propagation losses of about 0.2 dB/cm. No significant variation can be attributed to the different plasma etching processes used (sample G3 and G4). They cause a variation in the slope of the lateral edges, which are not critical because of the good confinement of the optical modes and the large width of the channel. On the contrary, the etching depth can play a key role, differences are observed between the propagation losses of samples G5 and G6. Sample G6, defined by plasma etching, results in a structure with a large confinement of the modes under the loaded area. This is caused by the removal of about 30 nm of Si_3N_4 (as shown by SEM) during the oxide plasma etching process. Hence the effective refractive index of the lateral cladding is lower for sample G6 than for sample G5, which in turn causes a better optical confinement.

In agreement with the simulated dependence of the modal confinement on the polarization state (not reported here), a polarization dependence of propagation losses has been measured by coupling-in polarized (TE or TM) light from a He–Ne laser (632.8 nm—5 mW). Moreover, propagation losses have been evaluated for the different optical modes by means of a selective excitation achieved by a fine control of the input angle and verifying the mode profile at the output

Table 1
Propagation losses at 780 nm as a function of geometry and fabrication

Samples	Waveguides	Propagation loss coefficient (dB/cm)	
		Cut-back	Top-view
G1	Rib (oxide plasma etcher)	2 ± 1	1.8 ± 0.2
G3	Channel (nitride plasma etcher)	0.2 ± 0.2	0.1 ± 0.05
G4	Channel (oxide plasma etcher)	0.3 ± 0.2	0.2 ± 0.2
G5	Strip-loaded (BHF wet etching)	2.5 ± 0.6	—
G6	Strip-loaded (oxide plasma etcher)	1.5 ± 0.2	1.4 ± 0.4

facet. Results are reported in Table 2 for waveguide G3 taken as representative sample. Similar results have been obtained also for the strip-loaded waveguide G6. An increase in the propagation loss coefficient with increasing the optical mode's order and a dependence on the polarization state is shown. It is worth noting that the TM losses are larger than TE ones. This difference is appreciable only for the higher order modes where propagation losses are larger. In fact, the increase of propagation losses as a function of the mode number is due to the increased scattering of light on the sidewalls of the channel.

Optical guided modes have also been measured in the near infrared range at 1544 nm. Fig. 5 shows the transmittance measured by the cut-back technique for the channel waveguide G3. From the linear fit results a propagation loss coefficient of about 4.8 ± 0.5 dB/cm. In Fig. 6, an example of a top-view measurement is shown for the strip-loaded waveguide G6. An exponential decay fit to the data (presented in linear scale) yields a propagation loss coefficient of 6.2 ± 0.5 dB/cm. The propagation loss coefficients of the different samples are reported in Table 3. Values obtained by the three different techniques are in good agreement.

Propagation losses at 1544 nm are quite larger than in the visible range and do not show substantial differences between the different waveguide geometries, though channel waveguides show lower propagation losses coefficient (about 4.5 dB/cm) than strip-loaded waveguides (about 6 dB/cm). The difference with the values obtained at 780 nm (Table 1) is mainly due to the poorer

confinement factor (20–40% as obtained by simulation at 1544 nm) of the optical mode and not due to absorption losses. In fact, the use of LPCVD technique results in low hydrogen content in the silicon nitride

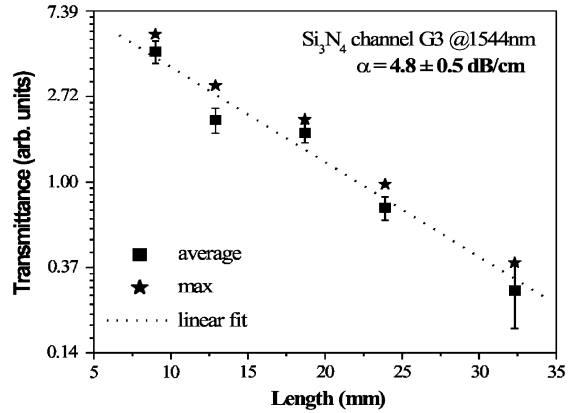


Fig. 5. Transmittance measurements as a function of the sample length (cut-back technique) of a channel waveguide (sample G3) at 1544 nm. The propagation loss coefficient is 4.8 ± 0.5 dB/cm.

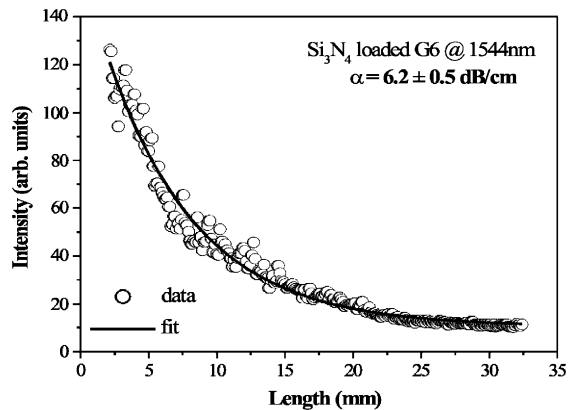


Fig. 6. Scattered light intensity (top-view measurements) along the sample length of a strip-loaded waveguide (sample G6) at 1544 nm. The propagation loss coefficient is 6.2 ± 0.5 dB/cm.

Table 2
Propagation losses at 632.8 nm as a function of guided mode and polarization for sample G3

Mode	Propagation loss coefficient (dB/cm)	Mode	Propagation loss coefficient (dB/cm)
TE ₀	0.2 ± 0.2	TE ₁₀	0.8 ± 0.2
TM ₀	0.3 ± 0.2	TM ₁₀	1.2 ± 0.2
TE ₁	0.2 ± 0.2	TE ₁₄	1.0 ± 0.2
TM ₁	0.3 ± 0.2	TM ₁₄	1.3 ± 0.2

Table 3
Propagation losses at 1544 nm as a function of geometry and fabrication

Samples	Waveguides	Propagation loss coefficient (dB/cm)		
		Cut-back	Top-view	Insertion losses
G3	Channel (nitride plasma etcher)	4.8 ± 0.5	4.3 ± 0.5	4.8 ± 1
G4	Channel (oxide plasma etcher)	—	4.9 ± 0.5	4.4 ± 1
G5	Strip-loaded (BHF wet etching)	—	4.1 ± 0.5	4.3 ± 1
G6	Strip-loaded (oxide plasma etcher)	5.8 ± 0.6	6.2 ± 0.5	6 ± 1

layer (as shown by IR absorption measurements, not reported here), reducing the absorption of the vibrational overtones of Si–H and N–H bonds.

The propagation losses values of our waveguides are within the state of the art of silicon nitride waveguides: 0.1 dB/cm for TE₀ mode at 632.8 nm has been reported in one of the earliest work on silicon nitride waveguiding film [9] and in more recent papers [15,16]; whereas higher values, about 0.3 and 0.6 dB/cm, have been reported at 632.8 nm on silicon nitride planar [13] and ridge-type waveguides, respectively [14]. It is worth noting that our results rely on the careful control and CMOS compatibility of the deposition process, and the reduced thickness of the silicon nitride core layer. To overcome the poor optical confinements in the IR range, mainly due to the thin core thickness, multi-layered waveguides have been designed and are in fabrication.

4. Conclusions

In this paper we have presented results on low-loss silicon-nitride waveguides fabricated within a CMOS pilot-line. All used processes are standard for microelectronics industry, which allow a good transferability of the reported results. We have fabricated and tested three different geometries of waveguides and found that channel waveguides show propagation losses of 0.1–0.2 dB/cm and with TE mode better guided (about 25–30%) with respect to TM mode in the visible range. In the infrared range, propagation losses are larger (about 4.5 dB/cm) and essentially due to the poor mode confinement within the thin core layer.

Acknowledgement

This work has been supported by PAT-FU.

References

- [1] Risch L. *Mater Sci Eng C* 2002;19:363.
- [2] Miller DAB. *Proc IEEE* 2000;88:728.
- [3] Haveman R. *Proceedings of workshop processing for ULSI: transistors to interconnects*, Austin, TX, 22 April, 1999.
- [4] Hibino Y. *IEICE Trans Commun E* 2000;83-B:2178.
- [5] Pavesi L. *J Phys Condens Matter Topical R* 2003;15:R1169.
- [6] Wong H. *Microelectronics Rel* 2002;42:317.
- [7] Moore SK. *Spectrum IEEE*, 31 July 2002.
- [8] Jang JH, Zhao W, Bae JW, Selvanathan D, Rommel SL, Adesida I. *Appl Phys Lett* 2003;83:4116.
- [9] Stutius W, Streifer W. *Appl Opt* 1977;16:3218.
- [10] Siriam S, Partlow WD, Liu CS. *Appl Opt* 1983;22:3664.
- [11] Henry CH, Kazarinov RF, Lee HJ, Orlovsky KJ, Katz LE. *Appl Opt* 1987;26:2621.
- [12] May P, Basu S, Chiu GL-T, Arjavalingham G. *IEEE J Lightwave Technol* 1990;8:235.
- [13] De Brabander GN, Boyd JT, Jackson HE. *IEEE J Quantum Electron* 1991;27:575.
- [14] Ohtani M, Hanabusa M. *Appl Opt* 1992;31:5830.
- [15] Inukai T, Ono K. *Japan J Appl Phys* 1994;33(5A):2593.
- [16] Bulla DAP, Borges BV, Romero MA, Morimoto NI, Neto LG, Cortes AL. *SBMO/IEEE MTT-S IMOC'99 proceedings*, 1999, p. 454.
- [17] de Ridder RM, Worhoff K, Driessen A, Lambeck PV, Albers H. *Special issue on silicon-based optoelectronics. IEEE J Selec Top Quantum Electron* 1998;4:930.
- [18] Netti C, Charlton MDB, Parker GJ, Baumberg JJ. *Appl Phys Lett* 2000;76:991.